Barrier Lypanunov Function-based Adaptive Control of an Ankle Exoskeleton

Yapeng Wang
Research Center of Satellite Technology
Harbin Institute of Technology
Harbin, China
Beijing Xinfeng Aerospace Equipment Co., Ltd.
Beijing, China
wangyapenghit@163.com

Yunhai Geng
Research Center of Satellite Technology
Harbin Institute of Technology
Harbin, China
gengyh@hit.edu.cn

Abstract—**The application of exoskeleton robots in industrial assembly and other fields plays a significant role in alleviating low back pain caused by work-related musculoskeletal disorders and improving work efficiency. Currently, the ankle joints of lower limb exoskeleton robots used in this field are all treated as passive joints. Ankle is important for weight-bearing joints of human lower limbs in the stability and flexibility of daily activities. To this end, the authors of this paper have designed a cable-driven ankle exoskeleton structure to achieve active dorsiflexion and plantarflexion movements in the sagittal plane. To compensate the modeling error and estimate the perturbation, neural network (NN) and nonlinear disturbance observer (NDO) are used. A time-varying barrier Lyapunov function is used to design an adaptive backtracking controller to constrain the system output error and ensure the tracking performance and safety of the robot. A healthy subject participates in the experiment wearing the cable-driven ankle exoskeleton. the experimental is conducted to validate performance of the proposed controller.**

Keywords—exoskeleton robot, ankle joint, adaptive control, cable-driven

I. Introduction

Work-related musculoskeletal disorders (WMSDs) is closely related to excessive physical load and specific work postures, which are particularly common in the manufacturing sector. These disorders not only affect the physical and mental health of operators but also result in significant economic losses [1]. Exoskeleton robots, as a type of human-robot interaction device, have been applied in various scenarios such as patient rehabilitation and assembly work. In assembly settings, the purpose of exoskeleton robots is to alleviate the muscle fatigue of assembly workers, thereby ensuring worker health and improving work efficiency. Scholars have conducted relevant studies and developed a series of prototype exoskeleton robots.

Among the exoskeletons mentioned above, which are used in the field of work assembly, a notable feature is that the hip and knee are actuated as active joints, while usually treating the ankle joint as a passive joint. However, ankle is important for weight-bearing joints of human lower limbs in the stability and flexibility of daily activities. [2, 3]. The ankle joint of the patient is prone to varus, foot drop and other spasms, which

seriously affect the patient's standing and walking; The ankle trochlear joint is prone to varus sprain in plantar flexion, and the patient's lack of strength increases the risk of sprain. The ankle joint provides 60% of the force for the gait during the lift, so training the joint for flexion is necessary. Therefore, the design of active ankle joint exoskeletons with driven mechanisms is of great significance for enhancing the application effects of exoskeletons used in the field of industrial assembly [4].

To this end, the authors of this paper have designed a cable-driven ankle exoskeleton structure to achieve active dorsiflexion and plantarflexion movements in the sagittal plane, as shown in Fig. 1. For such an exoskeleton robot, its motion control becomes another important issue.
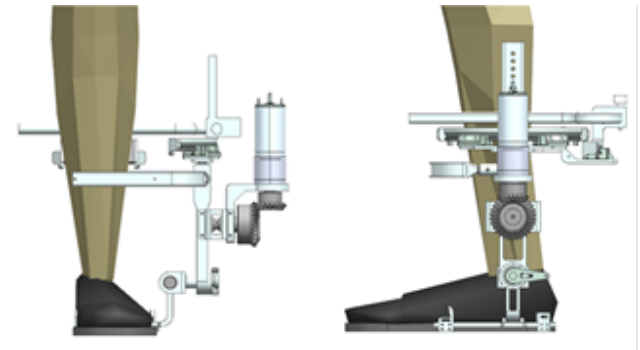

Fig. 1. 3D model of the cable-driven ankle exoskeleton robot for walking assistance.

The control of the ankle exoskeleton robot for walking assistance is important for human-robot coordination [5]. Proportional-integral-derivative (PID) controller [6] do not require complete dynamics of the exoskeleton robot, but it only operates suitably in regulation problems with limited performance. Another approach is using the controllers based on dynamic models. However, the model of exoskeleton robot is nonlinear, and the model parameters uncertainty influence the control performance. Furthermore, friction is also needed to be compensated [7]. In order to achieve friction compensation, a lot of dynamic friction models are built [8, 9] but these models need a calibration process [10], especially for complex mechanical structures, accurate friction models are difficult to

obtain. To overcome this problem, adaptive controller based on neural network (NN) has more obvious advantages [11]. Asl et al. compensated the unknown dynamics for a lower limb exoskeleton [12]. Therefore, NN is an effective way of dynamically compensation for the control of the proposed exoskeleton robot.

In addition to the fact that exoskeleton robots differ from ordinary industrial robots, it is necessary to consider the control issues caused by the human being within the control loop. [13]. The human body can be regarded as an unknown perturbation to the robot, which will affect the movement deviation of the robot. Using nonlinear disturbance observer (NDO) is a method to estimate above unknown perturbation [14]. At the same time, there is a relatively important human-robot safety problem, so the system output of the robot is constrained. Barrier Lypanunov function (BLF) is an effective way to deal with dynamic processes [15]. In terms of exoskeleton applications, tan-type BLF [16, 17] has been used. However, these algorithms are mainly used for upper limbs, not for lower limbs.

Therefore, in this paper for the proposed cable-driven ankle exoskeleton, a BLF-based adaptive controller is designed. The main contribution of the paper are as follows. An adaptive controller with time-varying tan-type BLF is proposed for cable-driven ankle exoskeleton robot. The overall framework of the control system is proposed and stability analysis is conducted. The experimental is conducted to validate performance of the proposed controller.

The rest of the paper is organized as follows. The problem formulation and preliminaries involved in the BLF-based adaptive controller is described in Section II . The BLF-based adaptive controller is designed and its stability is analyzed in Section III. Experiments are conducted in Section IV. Finally, the conclusion is presented in Section V.

II. PROBLEM FORMULATION AND PRELIMINARIES

A. System Descrption

The plantar flexion motion of the cable-driven ankle exoskeleton is the active movement, which is cable-driven as described in Fig. 1. The dorsiflexion is the passive movement achieved by the spring. The other movements of the ankle exoskeleton robot are in a free state to reduce and avoid the discomfort of the human lower limbs during gait and motivation. Aiming at the uncertainty of ankle rotation axis in different patients, a mechanism configuration with redundant degrees of freedom was proposed, which could realize the reachable working space in a small area. Aiming at the ankle joint prone to varus sprain, a four-link mechanism with variable stiffness was proposed. The scale parameters were designed and the spring stiffness was selected according to the gait data to realize the effects of small interference in the range of gait motion, large torque and limit position in the limit Angle. According to the joint torque during the gait process, the constrained spring stiffness in three rotation surfaces was selected respectively. The degree of freedom (DOF) and range of motion (ROM) for ankle exoskeleton robot are shown in Table I.

TABLE I.   DOF AND ROM OF THE ANKLE EXOSKELETON

DOF	ROM [deg]	Actuator
Dorsiflexion/Plantarflexion	-30~40	Active
Eversion/Inversion	-30~20	Passive
External/Internal rotation	-10~10	Passive

The ankle joint is a dorsiflexion/plantarflexion movement with single degree of freedom driven by the cable, in which the axis diameter of the cable pulling shaft is ra, the distance between the rotation center of joint and cable pulling shaft is la1, the distance between the rotation center of joint and the cable rotating shaft is la2, and the Angle of the ankle joint is θa (Fig. 2).
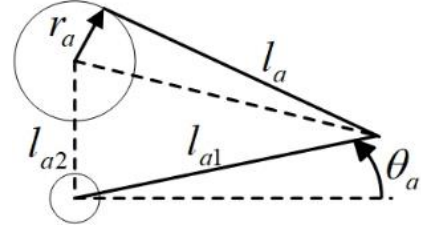

Fig. 2. Symbols in kinematic modeling.

If the change of the axis diameter caused by the change of the cable length during rotation is ignored, the length of the cable is satisfied

$$l_a = \sqrt{l_{a1}^2 + l_{a2}^2 + 2l_{a1}l_{a2}\sin\theta_a - r_a^2} \qquad (1)$$

The dynamical model is

$$M(\theta)\ddot{\theta} + C(\theta,\dot{\theta})\dot{\theta} + G(\theta) = \tau + \tau_d \qquad (2)$$

where M , C and G respectively represents the inertia, Coriolis and centripetal force, and the gravity term. τ is the actuation torque corresponding to the generalised coordinates. τ_d is total disturbance torque.

Property [18]: $\dot{M} - 2C$ is skew-symmetric. That is, $\forall y \in \mathbb{R}, (\dot{M} - 2C)y^2 = 0$.

Assumption: θ_d , $\dot{\theta}_d$ and $\ddot{\theta}_d$ are all bounded.

B. Preliminaries

The NDO algorithm allows the estimated disturbance $\hat{\tau}_d$ to track τ_d . Mohammadi et al proposes an NDO to eliminate acceleration measurements as followed [14]

$$\begin{cases} \dot{\varphi}_d = -LM^{-1}(z_d + Lx_2) + LM^{-1}(Cx_2 + G - u) \\ \hat{D} = \varphi_d + Lx_2 \end{cases} \qquad (3)$$

where $L \in \mathbb{R}$ is the gain coefficient.

The RBFNN can be represented as [19]

$$\phi(\mathbf{Z}_{NN}) = \mathbf{W}^T \varphi(\mathbf{Z}_{NN}) + \varepsilon(\mathbf{Z}_{NN}) \qquad (4)$$

where $\mathbf{Z}_{NN} \in \Omega \subset \mathbb{R}^m$ denotes the input vector. $\mathbf{W} \in \mathbb{R}^{l \times n}$ is weight matrix and l is the number of neuros. $\varphi(\mathbf{Z}_{NN}) = [\varphi_1(\mathbf{Z}_{NN}),\ldots,\varphi_l(\mathbf{Z}_{NN})]^T$ is the basic function of RBFNN and $\varphi_i(\mathbf{Z}_{NN})$ is the Gaussian function as

$$\varphi_i(\mathbf{Z}_{NN}) = \exp\left[\frac{-(\mathbf{Z}_{NN} - \mathbf{u}_i)^T (\mathbf{Z}_{NN} - \mathbf{u}_i)}{\sigma_i^2}\right], i = 1,\ldots,l \quad (5)$$

where $\mathbf{u}_i \in \mathbb{R}^m$ and σ_i respectively represents the center of the field and the width of the Gaussian function. For a sufficiently lager l, there exists an optimal weight matrix as $\mathbf{W}^*$ and an approximation error $\varepsilon^*(\mathbf{Z}_{NN})$ such that

$$\phi(\mathbf{Z}_{NN}) = \mathbf{W}^{*T}\varphi(\mathbf{Z}_{NN}) + \varepsilon^*(\mathbf{Z}_{NN}) \quad (6)$$

If the node center is appropriately chosen, then $\varepsilon^*(\mathbf{Z}_{NN})$ is bounded. The optimal matrix $\mathbf{W}^*$ is only used for analytical purpose and replaced by its estimation $\hat{\mathbf{W}}$ in practical systems. The estimation of $\phi(\mathbf{Z}_{NN})$ is described by

$$\hat{\phi}(\mathbf{Z}_{NN}) = \hat{\mathbf{W}}^T\varphi(\mathbf{Z}_{NN}) \quad (7)$$

And the estimation error is $\tilde{\mathbf{W}} = \mathbf{W}^* - \hat{\mathbf{W}}$. Thus

$$\phi(\mathbf{Z}_{NN}) - \hat{\phi}(\mathbf{Z}_{NN}) = \tilde{\mathbf{W}}^T\varphi(\mathbf{Z}_{NN}) + \varepsilon^*(\mathbf{Z}_{NN}) \quad (8)$$

III. BLF-BASED ADAPTIVE CONTROLLER DESIGN

The generalised variables are defined as $x_1 \triangleq \theta$ and $x_2 \triangleq \theta_d$ for practical applications and $x_{1d} \triangleq \theta_d$. Then, the state-space equation of (2) can be provided as follows:

$$\begin{cases} \dot{x}_1 = x_2 \\ \dot{x}_2 = -M^{-1}(Cx_2 + G - u - \tau_d) \end{cases} \quad (9)$$

The tracking error is $e_1 \triangleq x_1 - x_{1d}$ and $e_2 \triangleq x_2 - a_1$. $a_1 \in \mathbb{R}$ donates the auxiliary variable. Differentiating of e_1 yields to $\dot{e}_1 = x_2 - \dot{x}_{1d}$. Then a_1 is defined as

$$a_1 = -k_1 \frac{\rho^2}{\pi e_1} \tan\frac{\pi e_1^2}{2\rho^2} \cos^2\frac{\pi e_1^2}{2\rho^2}$$
$$-\frac{\dot{\rho}}{z_1}\left(\frac{2\rho}{\pi}\tan\frac{\pi e_1^2}{2\rho^2} - \frac{1}{\rho}e_1^2 \sec^2\frac{\pi e_1^2}{2\rho^2}\right)\cos^2\frac{\pi e_1^2}{2\rho^2} + \dot{x}_{1d} \quad (10)$$

A smooth and bounded performance function is defined as

$$\rho(t) \triangleq (\rho_0 - \rho_\infty)e^{-pt} + \rho_\infty \quad (11)$$

where ρ_0, ρ_∞ and p are all positive constant.

The BLF is considered as

$$V_1 = \frac{\rho^2}{\pi}\tan\frac{\pi e_1^2}{2\rho^2} \quad (12)$$

The time derivative of (12) along (10) is obtained as

$$\dot{V}_1 = -k_1 e_1^2 + e_2^T \Psi e_1 \quad (13)$$

where k_1 is control gains. And Ψ is a term, which is defined as $\Psi \triangleq \sec^2(2^{-1}\rho^{-2}\pi e_1^2)$.

With the avoidance of terms explosion, a first-order filter is designed

$$\tau_2 \bar{a}_1 + a_1 = \bar{a}_1, a_1(0) = \bar{a}_1(0) \quad (14)$$

here, $\tau_2 \in \mathbb{R}$.

Define the control torque as

$$\tau = -k_2 e_2 + M_n \dot{a}_1 + C_n a_1 + G_n + f - \tau_d - \Psi e_1 \quad (15)$$

where $f = \Delta M \dot{a}_1 + \Delta C a_1 + \Delta G$.

Applying RBFNN to approximate f as

$$f = \mathbf{W}^{*T}\varphi(\mathbf{Z}) + \varepsilon^*(\mathbf{Z}) \quad (16)$$

where $\mathbf{W}^*$ is the optimal metric. $\mathbf{Z} = [x_1^T \quad x_2^T \quad \alpha_1^T \quad \dot{\alpha}_1^T]^T$. $\bar{\varepsilon}_f$ are bounded, $\forall \mathbf{Z} \in \Omega_{\mathbf{Z}}$. The estimation can be written as $\hat{f} = \hat{\mathbf{W}}^T\varphi(\mathbf{Z})$. So the control torque in (14) can be written as

$$\tau = -k_2 e_2 + M_n \dot{a}_1 + C_n a_1 + G_n + \hat{\mathbf{W}}^T\varphi(\mathbf{Z}) - \hat{\tau}_d - \Psi e_1 \quad (17)$$

The dynamics can be written as

$$M\dot{e}_2 = -k_2 e_2 - Ce_2 + \tilde{\mathbf{W}}^T\varphi(\mathbf{Z}) - \varepsilon^*(\mathbf{Z}) + \tilde{\tau}_d - \Psi e_1 \quad (18)$$

where $\tilde{\tau}_d \triangleq \hat{\tau}_d - \tau_d$ and $\tilde{\tau}_d$ is bounded such that $\|\tilde{\tau}_d\| \le \bar{\tau}_d$.

The updating law is

$$\dot{\hat{\mathbf{W}}} = -\Gamma^{-1}\left(\varphi(e_2)^T + \ell\hat{\mathbf{W}}\right) \quad (19)$$

where Γ is positive constant. ℓ is positive constant.

The Lyapunov function is considered as

$$V_2 = \frac{1}{2}Me_2^2 \quad (20)$$

Using property and submitting (17) then

$$\dot{V}_2 = -k_2 e_2^2 + e_2 \tilde{\mathbf{W}}^T\varphi(\mathbf{Z}) - e_2 \varepsilon^*(\mathbf{Z}) - e_2 \tilde{\tau}_d - \Psi e_1 e_2 \quad (21)$$

Theorem: for the given robot system, if the controller is defined by (17), and updating law is designed by (19), $\theta(0)$ and $\dot{\theta}(0)$ satisfy certain conditions, then the proposed controller is stable with the adjustment of the control parameters and the close-loop system is robust.

Proof: The estimation error of (14) is $y_2 = x_{2d} - \bar{x}_2$. Thus, $\dot{x}_{2d} = -\tau_2^{-1}y_2$ and $\dot{y}_2$ can be rewritten using B_2, as followed

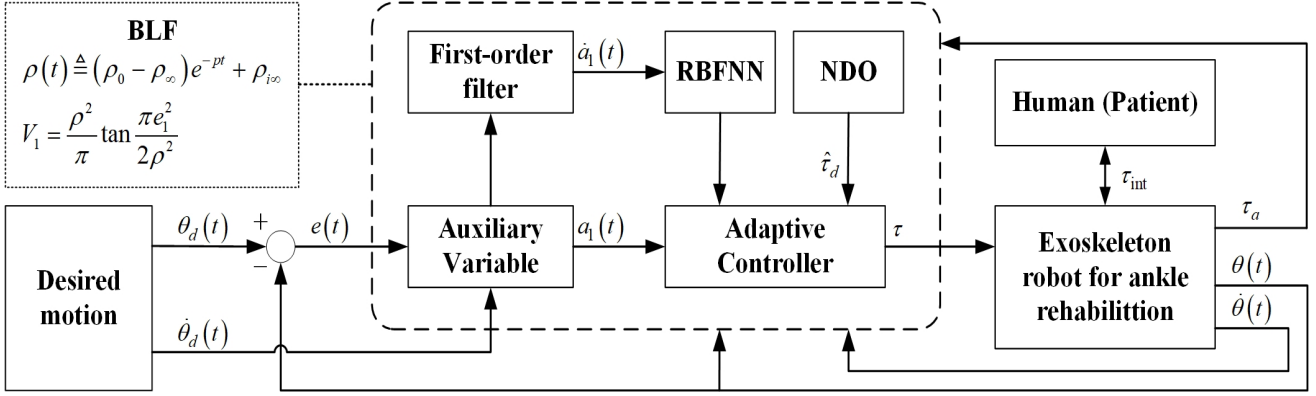$$\dot{y}_2 = -\frac{1}{\tau_2}y_2 + B_2(e_1, e_2, y_2, \ddot{x}_{1d}) \quad (22)$$

Fig. 3. Control diagram of the system.

The Lyapunov function is considered as follows

$$V = V_1 + V_2 + \frac{1}{2}tr\left(\tilde{\mathbf{W}}^T\mathbf{\Gamma}^{-1}\tilde{\mathbf{W}}\right) + \frac{1}{2}y_2^T y_2 \qquad (23)$$

Then, the derivative of (23) is

$$\dot{V} = -k_1 e_1^2 - k_2 e_2^2 + \frac{2\rho\dot{\rho}}{\pi}\tan\frac{\pi e_1^2}{2\rho^2} - tr\left(\ell\tilde{\mathbf{W}}^T\hat{\mathbf{W}}\right)$$
$$-e_2\varepsilon^* - e_2\tilde{\tau}_d + y_2\left(-\frac{1}{\tau_2}y_2 + B_2\right) \qquad (24)$$

And then

$$-\tilde{\mathbf{W}}^T\hat{\mathbf{W}} \le -\frac{1}{2}\tilde{\mathbf{W}}^T\tilde{\mathbf{W}} + \frac{1}{2}\mathbf{W}^{*T}\mathbf{W}^* \qquad (25)$$

$$-e_2\varepsilon^* \le e_2^2 + \frac{1}{2}\varepsilon^{*2} \le e_2^2 + \frac{1}{2}\|\varepsilon^*\|^2 \qquad (26)$$

$$-e_2\tilde{\tau}_d \le e_2^2 + \frac{1}{2}\tilde{\tau}_d^2 \le e_2^2 + \frac{1}{2}\overline{\tau}_d^2 \qquad (27)$$

Then (24) can be derived

$$\dot{V} \le -k_1 e_1^2 - (k_2-1)e_2^2 - \frac{1}{\tau_2}y_2^2 - \frac{1}{2}\ell tr\left(\tilde{\mathbf{W}}^T\tilde{\mathbf{W}}\right) + B \qquad (28)$$

where $B = 2^{-1}\overline{\tau}_d^2 + 2^{-1}\ell tr\left(\mathbf{W}^{*T}\mathbf{W}\right) + 2^{-1}\|\varepsilon^*\|^2$.

Then, a calculation is haven as

$$\dot{V} \le -\lambda V + B \qquad (29)$$

The proposed controller is stable with the adjustment of the control parameters λ and the close-loop system is robust. The control diagram is shown in Fig. 3.

IV. EXPERIMENTAL RESULTS

The performance of the proposed NN-based adaptive controller (NNAC) was evaluated. A healthy subject participated (age: 28, weight: 80kg. height: 185cm) in the experiment wearing the exoskeleton robot (Fig. 4). The subject walked on a treadmill wearing the proposed ankle exoskeleton.

The desired ankle motion path is obtained by parameterized generation method [20]. A total of $N = 7^4$ nodes were chosen for RBFNN-based adaptive controller. The centers are evenly distributed in

$\begin{bmatrix} -1.5 & -1.0 & -0.5 & 0 & 0.5 & 1.0 & 1.5 \end{bmatrix}$ and $\sigma = 50$ in (9). Parameters of updating laws were $\Gamma = 0.01$ and $\ell = 0.01$. Control gain for NDO was chosen as $\mathbf{X} = 0.02$. The control gains were $k_1 = 10$, $k_2 = 90$ and $\tau_2 = 0.005$. The parameters in (15) were selected as $\rho_0 = 10\,\text{deg}$, $\rho_\infty = 2.5\,\text{deg}$ and $p = 1$, that is, the final tracking error range is within 2.5 deg. A PID controller was compared with the proposed NNAC in the article.

Fig. 4. The participator wearing the exoskeleton robot.

The experimental results have been shown in Figs. 5-6 and Table II. Fig 5 shows desired trajectory for ankle exoskeleton robot during a gait cycle. The comparison by the maximum absolute error (MAE) and integral of absolute error (IAE) [21] has been shown in Table II and Fig. 6. According to the results shown in Table II, the NNAC has smaller MAE and IAE than the PID controller, which obviously validates the performance of the NNAC. Better control performance can be obtained after a more proper design of the control parameters in PID controller. However, the predefined output constraints may be violated in the comparison experiment as shown in Fig. 6. Under the action of proposed NNAC, the tracking error gradually converges to a certain range. According to results, the NNAC can meet the requirements of walking assistance.

TABLE II. COMPARISON OF NNAC AND PID CONTROLLER

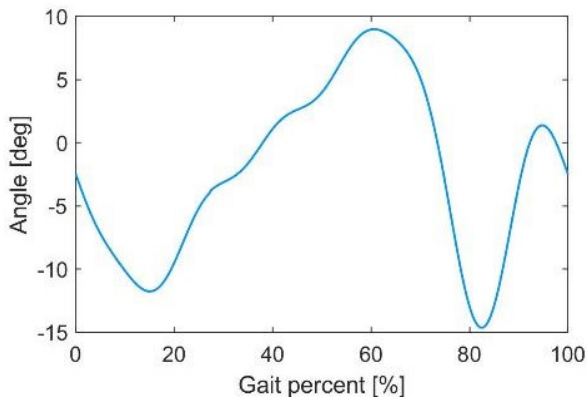| Controller	MAE [deg]	IAE [deg]
NNAC	2.2724	0.6256
PID	3.2979	0.8970

Fig. 5. Desired trajectory for ankle exoskeleton robot during a gait cycle.
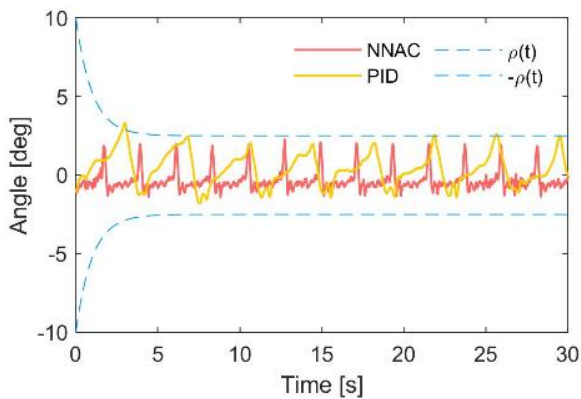

Fig. 6. Tracking error with different controllers.

V. CONCLUSION

To compensate the modeling error and estimate the perturbation, NN-based NDO is used. A time-varying barrier Lyapunov function is used to design an adaptive backtracking controller to constrain the system output error and ensure the tracking performance and safety of the robot. A healthy subject participates in the experiment wearing the cable-driven ankle exoskeleton. The experimental is conducted and the performance of the proposed controller is compared with a PID controller.

REFERENCES

[1] B. R. Theodore, T. G. Mayer, and R. J. Gatchel, "Cost-effectiveness of early versus delayed functional restoration for chronic disabling occupational musculoskeletal disorders," *Journal of occupational rehabilitation,* vol. 25, pp. 303-315, 2015.

[2] M. W. Whittle, *Gait analysis: an introduction*: Butterworth-Heinemann, 2014.

[3] D. A. Neumann, *Kinesiology of the musculoskeletal system: foundations for rehabilitation*: Elsevier Health Sciences, 2013.

[4] L. Mo, P. Feng, Y. Shao *et al.*, "Anti-disturbance sliding mode control of a novel variable stiffness actuator for the rehabilitation of neurologically disabled patients," *Frontiers in Robotics and AI,* vol. 9, pp. 864684, 2022.

[5] D. Shi, L. Wang, Y. Zhang *et al.*, "Review of human-robot coordination control for rehabilitation based on motor function evaluation," *Frontiers of Mechanical Engineering,* vol. 17, no. 2, pp. 28-31, 2022.

[6] Z. Chen, Q. Guo, H. Xiong *et al.*, "Control and implementation of 2-DOF lower limb exoskeleton experiment platform," *Chinese Journal of Mechanical Engineering,* vol. 34, no. 1, pp. 1-17, 2021.

[7] F. Qin, H. Zhao, S. Zhen *et al.*, "Adaptive robust control for lower limb rehabilitation robot with uncertainty based on Udwadia–Kalaba approach," *Advanced Robotics,* vol. 34, no. 15, pp. 1012-1022, 2020.

[8] L. Márton, and B. Lantos, "Control of mechanical systems with Stribeck friction and backlash," *Systems & Control Letters,* vol. 58, no. 2, pp. 141-147, 2009.

[9] R. M. Hirschorn, and G. Miller, "Control of nonlinear systems with friction," *IEEE Transactions on Control Systems Technology,* vol. 7, no. 5, pp. 588-595, 1999.

[10] M. Saadatzi, D. C. Long, and O. Celik, "Comparison of human-robot interaction torque estimation methods in a wrist rehabilitation exoskeleton," *Journal of Intelligent & Robotic Systems,* vol. 94, no. 3, pp. 565-581, 2019.

[11] P. M. Patre, W. MacKunis, K. Kaiser *et al.*, "Asymptotic tracking for uncertain dynamic systems via a multilayer neural network feedforward and RISE feedback control structure," *IEEE Transactions on Automatic Control,* vol. 53, no. 9, pp. 2180-2185, 2008.

[12] H. J. Asl, K. Katagiri, T. Narikiyo *et al.*, "Satisfying task completion and assist-as-needed performance in robotic exoskeletons," *IEEE Transactions on Medical Robotics and Bionics,* vol. 3, no. 3, pp. 791-800, 2021.

[13] Y. Ding, M. Kim, S. Kuindersma *et al.*, "Human-in-the-loop optimization of hip assistance with a soft exosuit during walking," *Science Robotics,* vol. 3, no. 15, pp. eaar5438, 2018.

[14] A. Mohammadi, M. Tavakoli, H. J. Marquez *et al.*, "Nonlinear disturbance observer design for robotic manipulators," *Control Engineering Practice,* vol. 21, no. 3, pp. 253-267, 2013.

[15] X. Jin, "Nonrepetitive trajectory tracking for nonlinear autonomous agents with asymmetric output constraints using parametric iterative learning control," *International Journal of Robust and Nonlinear Control,* vol. 29, no. 6, pp. 1941-1955, 2019.

[16] Q. Wu, Z. Wang, Y. Chen *et al.*, "Barrier Lyapunov function-based fuzzy adaptive admittance control of an upper limb exoskeleton using RBFNN compensation," *IEEE/ASME Transactions on Mechatronics,* vol. 10.1109/TMECH.2024.3392604, 2024.

[17] Z. Li, B. Huang, A. Ajoudani *et al.*, "Asymmetric bimanual control of dual-arm exoskeletons for human-cooperative manipulations," *IEEE Transactions on Robotics,* vol. 34, no. 1, pp. 264-271, 2017.

[18] J.-J. E. Slotine, and W. Li, *Applied nonlinear control*: Prentice hall Englewood Cliffs, NJ, 1991.

[19] J. Park, and I. Sandberg, "Universal approximation using radial-basis-function networks," *Neural Computation,* vol. 3, no. 2, pp. 246-257, 2014.

[20] D. Shi, W. Zhang, X. Ding *et al.*, "Parametric generation of three-dimensional gait for robot-assisted rehabilitation," *Biology Open,* vol. 9, pp. 047332, 2020.

[21] Y. Cao, and J. Huang, "Neural-network-based nonlinear model predictive tracking control of a pneumatic muscle actuator-driven exoskeleton," *IEEE/CAA Journal of Automatica Sinica,* vol. 7, no. 6, pp. 1478-1488, 2020.